Isotactic Polypropylene-Based Stereoregular Diblock Copolymers: Syntheses and Self-Assembly

Jing-Chung Kuo, Wen-Fu Lin, Chia-Hue Yu, and Jing-Cherng Tsai*

Department of Chemical Engineering, National Chung Cheng University, Chia-Yi 62142, Taiwan

Tzu-Chung Wang, Tsai-Ming Chung, and Rong-Ming Ho*

Department of Chemical Engineering, National Tsing Hua University, Hsinchu 30013, Taiwan

Received April 1, 2008; Revised Manuscript Received July 14, 2008

ABSTRACT: The preparation of polyolefin-based stereoregular diblock copolymers (BCPs) by postpolymerization of hydroxy-capped isotactic polypropylene (iPP) led to the successful generation of a series of structurally well-defined iPP-based stereoregular BCPs for self-organizing into various nanostructures. The hydroxy-capped iPP prepolymer was synthesized by using *ansa*-metallocene catalysts to mediate the selective chain transfer to alkylaluminums during isospecific polymerization of propylene, leading to the production of alkylaluminum end-capped iPP as the preliminary product. Subsequently, in-situ O_2/H_2O_2 treatment of the resulting aluminum-capped iPP led to the successful preparation of hydroxy-capped iPP. The terminal hydroxyl end group of the iPP-based prepolymer was allowed to undergo tosylation reaction that led to the production of tosyl group end-capped iPP with a quantitative functional group conversion ratio. Subsequently, coupling the tosyl group end-capped iPP with living anionic poly(2-vinylpyridine) (P2VP) provided a series of structurally well-defined iPP-based BCPs. Various microphase-separated nanostructures can be obtained by taking advantage of the synthesized stereoregular BCPs for self-assembly. Furthermore, an interesting phase transformation from cylinder phase with hexagaonal packing to gyroid phase with bicontinuous structure can be induced by shearing the samples at the ordered melt state.

Introduction

Block copolymers (BCPs) are characterized by their chemical structures of combining two or more chemically distinct polymer segments that are covalently strung together.[1] Because of these unique structures, structurally well-defined BCPs are able to self-organize into ordered nanopatterns.[2] Incorporating crystallizable moieties within BCPs has been demonstrated to further increase the morphological richness and kinetic complexity in the self-assembly studies.[3] A recent report further revealed that the incorporation of stereoregular segments into BCPs can result in the formation of unusual nanopatterns due to the stereointeraction between stereoregular entities.[4] Despite this, simultaneous investigation of stereointeraction and crystallization behavior in the molecular level by using stereoregular semicrystalline BCPs has been extremely limited due to the difficulties in the preparation of stereoregular BCPs.

To date, stereoregular polyolefin-based BCPs can be prepared mainly by two synthetic routes: (i) conduct of living polymerization in the presence of stereospecific catalysts,[5] in which the BCPs are generated directly by sequential polymerizations of different monomers, and (ii) utilization of stereoregular polymers with end groups (end-functionalized stereoregular prepolymers) that can be linked to the second polymer block by postpolymerization.[6] In this vein, the development of novel catalyst systems to induce living stereospecific polymerization (route i, Scheme 1) has been receiving considerable attention and progress in recent years because living polymerizations offer a direct linking method for connecting different polymer blocks.[5] Unfortunately, restrictions on monomers that are able to undergo living polymerizations hamper the utilization of this synthetic route for preparing suitable stereoregular BCPs, which possess the desired architecture with sufficient segregation strength between different blocks for microphase separation.[1,5] In contrast, the potential of connecting a broad variety of polymer segments onto the end-functionalized stereoregular prepolymer (route ii, Scheme 1) offers the tantalizing prospect of producing various stereoregular BCPs with tuning segregation strength in the second block.[7] Nevertheless, the syntheses of stereoregular BCPs via the end-functionalized prepolymer route would encounter the difficulties in providing the stereoregular BCPs with a well-defined chemical structure (e.g., uniform chemical structure with a narrow range of molecular weight distribution). In order to overcome these synthetic difficulties, the preparation of stereoregular BCPs has to start from a structurally well-defined stereoregular end-functionalized prepolymer for ensuring its uniform domain size in the stereoregular block. In addition, the stereoregular end-functionalized prepolymer needs to have a highly reactive terminal functional group for providing an efficient linkage for connecting onto other polymer blocks. Since stereoregular end-functionalized polymer can only be prepared by limited methods (via employing stereoregular catalyst to mediate the selective chain transfer reaction during stereospecific polymerization of α-olefins),[8] suitable stereoregular end-functionalized prepolymer is extremely difficult to obtain.

The preparation of hydroxy-capped polyolefins, including hydroxy-terminated poly(methylene-1,3-cyclopentane) and polyethylene, via the use of a bulky metallocene catalyst (i.e., Cp^*ZrCl_2, $Cp^* = \eta^5\text{-}C_5Me_5$) to mediate the selective chain transfer to aluminum drew our attention. These synthetic routes offered the introduction of a terminal hydroxyl functional group for use as the reactive terminal group to conduct BCP syntheses.[9,10] Prior reports showed that employing isospecific metallocene catalysts to mediate alkylaluminum transfer during propylene polymerization did not lead to the selective production of hydroxy-capped iPP as the formation of other chain end structures by involving different chain transfer pathways also occurred.[11] In this study, we demonstrate that the pure hydroxy-capped isotactic polypropylene (OH-capped iPP) can be selec-

* To whom correspondence should be addressed. Tel 886-5-2720411ext 33460, Fax 886-5-2721206, e-mail chmjct@ccu.edu.tw (J.-C.T.); Tel 886-3-5738349; Fax 886-3-5715408; e-mail rmho@mx.nthu.edu.tw (R.-M.H.).

10.1021/ma8007288 CCC: $40.75
Published on Web 10/10/2008

Scheme 1

Route *i* : stereospecific living polymerization

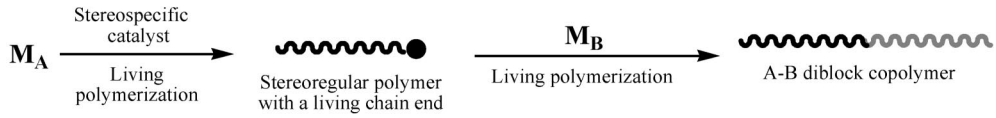

Route *ii* : post-polymerization of stereoregular prepolymer

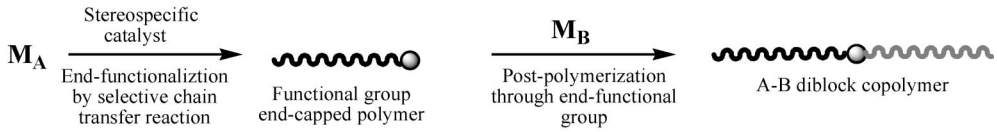

M_A: monomer A; M_B: monomer B; ● : living polymerization catalyst ○ : functional group

Table 1. Selective Chain Transfer Reaction Studied by Coordination Propylene Polymerization Propylene in the Presence of Various Alkyaluminums and Metallocene Catalysts[a]

						crude iPP polymer				end-groups ratio (%)[g]		
entries	catalyst[b]	AlR_3[c]	AlR_3 (mmol)	press. (bar)	temp (°C)	activity[d]	M_n[e]	PDI[e]	T_m (°C)[f]	hydroxyl	vinylidene	2-butenyl
1	I	TMA	5	0.6	60	3900	9400	1.96	116.28	10.60	78.73	10.67
2	I	TMA	5	0.6	30	2890	16800	1.77	124.31	22.76	59.98	17.26
3	I	TMA	5	0.6	0	1960	32200	1.82	147.94	28.46	51.22	20.32
4	I	TEA	5	0.6	60	3960	5900	1.90	131.21	17.52	81.32	1.16
5	I	TEA	5	0.6	30	2720	8270	1.86	132.56	32.17	63.39	4.44
6	I	TEA	5	0.6	0	1760	13800	1.71	139.78	42.17	52.20	5.63
7	I	TIBA	5	0.6	30	4510	21200	1.75	138.54	0.72	89.42	9.86
8	II	TMA	5	0.6	30	2200	10300	1.67	122.36	10.25	65.56	24.19
9	II	TMA	5	0.6	0	1770	16300[f]	1.69	137.58	14.38	57.35	28.27
10	II	TEA	5	0.6	30	2120	6500	1.71	120.17	15.43	72.33	12.24
11	II	TEA	5	0.6	0	1210	9800	1.80	138.40	20.76	61.90	17.34
12	III	TMA	5	0.6	60	3480	7500	2.11	107.89	45.89	37.32	16.79
13	III	TMA	5	0.6	30	2510	10100	1.82	111.09	65.56	22.19	12.25
14	III	TMA	5	0.6	0	1610	15000[f]	1.61	147.31	77.69	13.54	8.77
15	III	TEA	5	0.6	60	2300	3900	1.80	124.12	91.50	7.22	1.28
16	III	TEA	5	0.6	30	1660	5200	1.77	133.25	96.87	2.78	0.35
17	III	TEA	5	0.6	0	1220	8700	1.65	128.85	98.42	~1.58	
18	III	TEA	5	0.3	0	1130	7200	1.63	125.26	>99		
19	III	TEA	10	0.3	0	990	5400	1.77	131.43	>99		
20	III	TEA	15	0.3	0	630	2100	1.89	124.56	>99		
21	III	TEA	20	0.3	0	420	1300	1.93	117.45	>99		
22	III	TEA	25	0.3	0	310	1000	1.87	114.60	>99		

[a] Polymerization conditions: 50 mL of toluene; 5 μmol of zirconium catalyst; 5 mmol of MAO; reaction time = 1 h. [b] I = *rac*-$(CH_3)_2Si(Ind)_2ZrCl_2$/MAO; II = *rac*-$(CH_3)_2C(Ind)_2ZrCl_2$/MAO; III = *rac*-$C_2H_4(Ind)_2ZrCl_2$/MAO. [c] TMA = trimethylaluminum, TEA = triethylaluminum, and TIBA = triisobutylaluminum. [d] Catalytic activity = kg of polymer/(mol of catalyst h). [e] M_n (number-average molecular weight), M_w (weight-average molecular weight), and PDI (polydispersity, M_w/M_n) were determined by high-temperature GPC (solvent 1,2,4-trichlorobenzene; temperature 135 °C). [f] T_m (melting temperature) was determined by DSC. [g] The end-group ratios were determined by ^1H NMR analyses.

tively generated via the proper selection of isospecific metallocene catalysts and alkyaluminums (chain transfer agents). As a result, using the hydroxyl end group of the OH-capped iPP to undergo subsequent block copolymerization reactions affords structurally well-defined iPP-based stereoregular BCPs. A variety of self-assembled nanostructures can be obtained in the self-assembly of the iPP-based stereoregular BCPs. Among the ordered phases resulting from the microphase separation of BCPs, a gyroid phase in BCPs has been exploited for potential applications involving charge transport, photonic materials, and membrane reactors because of its unique bicontinuous structure. While the preparation of nanoporous materials from ordered BCPs forming the gyroid phase has been demonstrated or suggested, only thin films and/or poorly efficient (or chemically harsh) methods have been used. Also, the microphase-separated gyroid structure with a macroscpic scale could be used for many engineering applications, such as scaffold. Here we aim to prepare a gyroid nanostructure from the self-assembly of the well-defined iPP-based stereoregular BCPs with a high functionality matrix phase, such as poly(2-vinylpyridine) (P2VP), because of the coordination between the nitrogen lone-pair electrons and inorganic precursors. We anticipate that the marriage of iPP block and P2VP block for the formation of ordered three-dimensional bicontinuous phase can be used to enrich the functionality and complexities of the BCPs in the applications of nanotechnologies.

Experimental Section

General Procedure. All reactions and manipulations were conducted under a nitrogen atmosphere using the standard Schlenk line or drybox techniques. Solvents and common reagents were commercially obtained and were used either as received or purified by distillation with sodium/benzophenone. Propylene (purity >99.9%) and oxygen (purity >99%) were obtained from Matheson and were used as received. *N*-Butyllithium (1.6 M in hexane) and *p*-toluenesulfonyl chloride (99%) were purchased from Aldrich and

Scheme 2

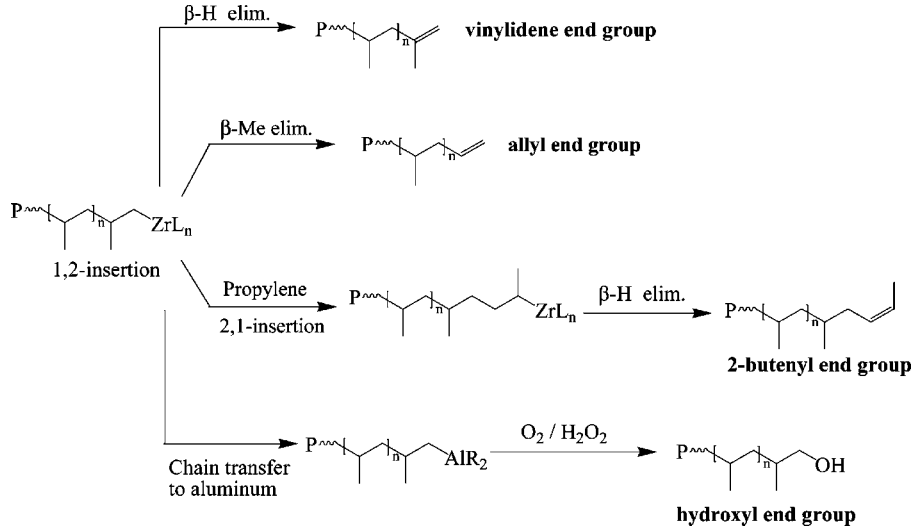

were used as received. The 2-vinylpyridine (97%), purchased from Aldrich, was dried over calcium hydride and distilled under vacuum before use. $C_2H_4(Ind)_2ZrCl_2$ (III), purchased form Aldrich, was used as received. $(CH_3)_2Si(Ind)_2ZrCl_2$ (I)[12] and $(CH_3)_2C(Ind)_2ZrCl_2$ (II)[13] were synthesized using the method described in the literature. Trimethylaluminum (TMA, 2 M solution in hexane), triethylaluminum (TEA, 1 M solution in hexane), and triisobutylaluminum (TIBA, 1 M solution in toluene) were purchased from Aldrich and were used as received. Methylaluminoxane (MAO, 14% in toluene), purchased from Albemarle, was dried under vacuum to remove residual TMA.[14] The resulting TMA-free MAO was diluted in toluene to the desired concentration before used.

Preparations of OH-Capped iPP. Representative experiment (for entry 19 of Table 1): A 250 mL stainless steel reactor, equipped with a magnetic stirrer, was allowed to dry at 80 °C under vacuum. After refilled with nitrogen, the reactor was cooled to 0 °C and was then charged sequentially with 50 mL of toluene, 5.0 mol of MAO (in toluene), and 5.0 mol of *rac*-$C_2H_4(Ind)_2ZrCl_2$. After allowing the reactor to stir at 0 °C for 5 min, the reactor was charged with 10.0 mmol of TEA and then with propylene (0.3 bar) to initiate the polymerization reaction. Polymerization was conducted at 0 °C for 1 h, after which the propylene was discharged from the reactor. The polymer solution was then treated with oxygen at a flow rate of 12 mL/min for 1 h. After that, the solution was slowly warmed to room temperature and was then charged with H_2O_2 (2 mL, 30% in H_2O). After stirring the solution at room temperature for 30 min, the solution was treated with excess methanol (ca. 40 mL), which led to the deposition of end-functionalized isotactic polypropylene (iPP) as a white precipitate. The resulting polymer was isolated after filtration and dried under vacuum to provide 4.94 g of OH-capped iPP. M_n = 5400 g/mol, M_w/M_n = 1.77 by GPC (in 1,2,4-trichlorobenzene at 135 °C).

Soxhlet Extraction of OH-Capped iPP in THF.[15,16] On a vacuum line, 4.94 g of OH-capped iPP (M_n = 5400 g/mol, M_w/M_n = 1.77, entry 19 of Table 1) was placed in a Soxhlet extractor and was allowed to undergo Soxhlet extraction in boiling THF (80 mL)

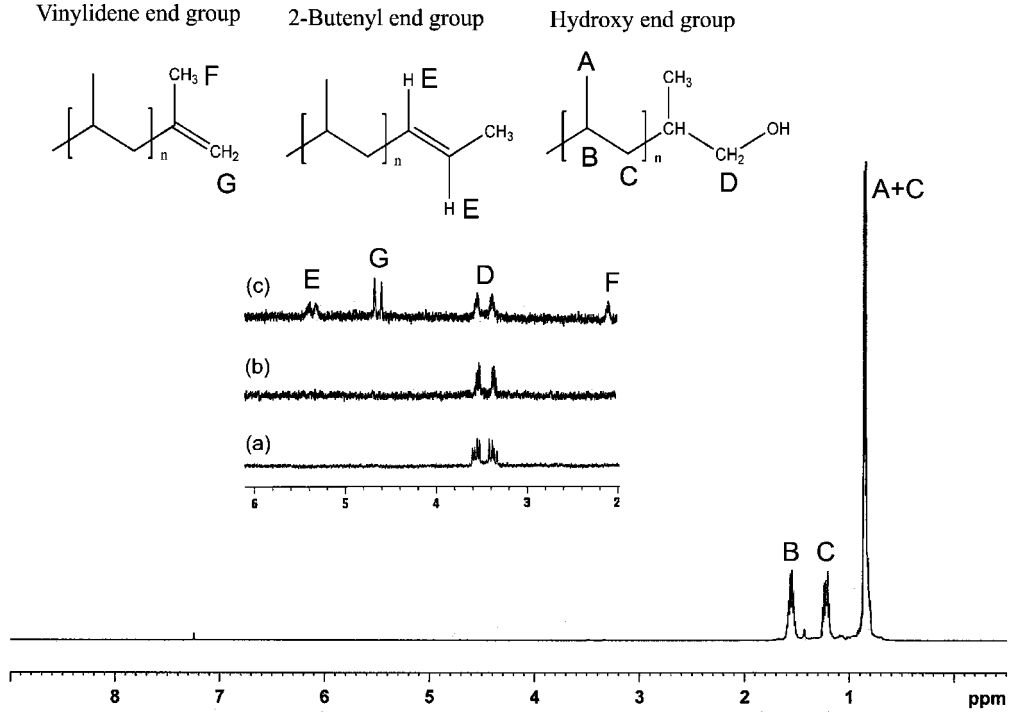

Figure 1. Expanded ^{1}H NMR (500 MHz) region of various iPP samples (a) M_n = 5400 g/mol, M_w/M_n = 1.77 (entry 19 of Table 1), (b) M_n = 5200 g/mol, M_w/M_n = 1.77 (entry 16 of Table 1), (c) M_n = 7500 g/mol, M_w/M_n = 2.11 (entry 12 of Table 1) (solvent, $CDCl_3$; temperature 60 °C).

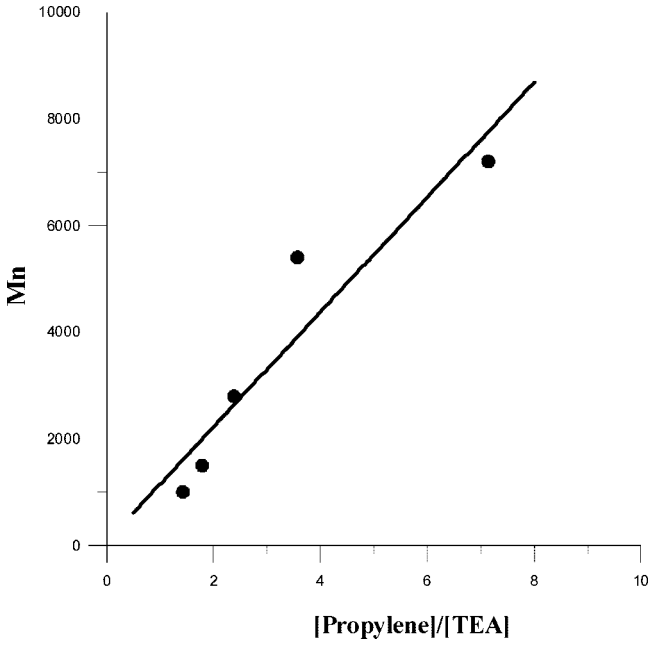

Figure 2. Plots of number-average molecular weight (M_n) of OH-capped iPP vs the mole ratios of [propylene]/[TEA] prepared by *rac*-$C_2H_4(Ind)_2ZrCl_2$/MAO at 0 °C using TEA as the chain transfer agent (entries 18−22 of Table 1).

for 24 h. The resulting THF solution was collected and was allowed to concentrate under vacuum to 10 mL. The resulting solution was then charged with excess methanol (ca. 20 mL), which in turn resulted in the deposition of the lower molecular weight, THF-soluble OH-capped iPP as a white precipitate. The resulting THF soluble polymer was isolated by filtration and dried under vacuum to provide 1.24 g of OH-capped iPP [M_n = 2820 g/mol, M_w/M_n = 1.50 by GPC (in 1,2,4-trichlorobenzene at 135 °C); isotacticity (mmmm) = 76% by ^{13}C NMR[17] (solvent $CDCl_3$; temperature 60 °C)].

Preparation of Tosyl Group End-Capped iPP. A 200 mL three-neck round-bottom flask, equipped with a magnetic stirrer, was charged with 1.0 g of the THF soluble OH-capped iPP (M_n = 2820 g/mol, M_w/M_n = 1.50) and with 50 mL of heptane. The resulting solution was allowed to stir at room temperature and was then charged with excess (3.2. mmol) of *n*-butyllithium. The resulting solution was slowly heated to 60 °C and was then charged with 0.61 g of *p*-toluenesulfonyl chloride (3.2 mmol). The tosylation reaction was conducted at 60 °C for 24 h. After that, the solution was allowed to concentrate to 10 mL by removing volatiles under vacuum. The resulting polymer solution was charged with excess methanol (ca. 10 mL), and this led to the deposition of tosyl group end-capped iPP as an off-white precipitate. The resulting precipitate was washed with acetone, isolated by filtration, and dried under vacuum for 24 h to provide 1.01 g of tosyl group end-capped iPP [M_n = 2860 g/mol, PDI = 1.50, determined by high-temperature GPC (in 1,2,4-trichlorobenzene at 135 °C)].

Preparation of iPP-*b*-P2VP. On a vacuum line, 0.5 g of tosyl group end-capped iPP (M_n = 2860 g/mol, M_w/M_n = 1.50) was dissolved in 50 mL of toluene at 50 °C. The solution was then cooled to room temperature and was charged with excess (ca. 0.4 mmol) of freshly prepared living anionic P2VP (M_n = 4220 g/mol, M_w/M_n = 1.07). Subsequently, the solution was slowly warmed to 50 °C and was then maintained at 50 °C for 12 h. After that, the polymer solution was quenched with excess methanol (ca. 20 mL), and this led to the deposition of the polymer mixture as a white precipitate. The resulting polymer mixture (containing iPP-*b*-P2VP, the excess P2VP, and the residual tosyl group end-capped iPP) was isolated after filtration and dried under vacuum. The purification of the iPP-*b*-P2VP BCPs was completed in two steps. First, the excess P2VP (soluble in boiling methanol) was removed by Soxhlet extraction in boiling methanol. The resulting methanol insoluble fraction was collected, dried, and allowed to undergo a second Soxhlet extraction with heptane to remove the residual tosyl group end-capped iPP. The resulting heptane-insoluble fraction was collected and dried under vacuum overnight to provide 0.87 g of iPP-*b*-P2VP as a white solid. M_n = 8020 g/mol, M_w/M_n = 1.10 by GPC (in 1,2,4-trichlorobenzene, at 135 °C).

Polymer Analysis. Molecular weight and MWD (M_w/M_n) were determined through high-temperature gel permeation chromatography (Waters 150-CALAC/GPC) with a refractive index (RI) detector and a set of U-Styragel HT columns of 10^6, 10^5, 10^4, and 10^3 pore sizes in series. The measurements were taken at 135 °C using 1,2,4-trichlorobenzene as solvent. PS samples with narrow MWDs were used as the standards for calibration. The standards were in the range of absolute molecular weight, which is from 980 to 2 110 000; the *R* square of the ideal calibrated line was limited to up to 0.999.

The ^1H (500 MHz) and ^{13}C NMR (500 MHz) spectra were recorded on a Bruker AV-500 NMR spectrometer. The iPP-based samples were dissolved into $CDCl_3$ or benzene-d_6 as solvents. The recorded temperature was at 40−80 °C.

Bulk Sample Preparation. The bulk samples were subjected to a large-amplitude oscillating shear at 150 °C. The shear apparatus was aerated with nitrogen gas to prevent thermal degradation. The shear direction was along the *x* direction, and the shear gradient was along the *z* direction. The shear frequency was 0.5 Hz, and the shear amplitude was 150%. To eliminate any residual stresses on microdomains (MD) during the shearing process, all oriented bulk samples were annealed for 12 h at 140 °C, which is well above the glass transition temperature of P2VP block ($T_{g,P2VP}$ = 60.4 °C) and the melting temperature of iPP block ($T_{m,iPP}$ = 108.4 °C), and then quenched the samples to 40 °C for isothermal crystallization under a nitrogen atmosphere.

Differential Scanning Calorimeter (DSC). DSC experiments were carried out by using the Perkin-Elmer DSC 7 system to measure the thermal behaviors (e.g., the melting point and glass transition temperature) of the iPP-*b*-P2VP. The DSC thermograms were recorded during the second heating cycle from −40 to 180 °C with a heating rate of 10 °C /min after cooling by 10 °C/min from the ordered melt state of samples at 180 °C.

Transmission Electron Microscopy (TEM). Microsections of iPP-*b*-P2VP bulk samples having thickness about 40 nm were obtained by ultramicrotomy using a Reichert Ultracut microtome. Bright field TEM images were obtained by using mass−thickness contrast with a JEOL TEM-1200x transmission electron microscope (at an accelerating voltage of 120 keV). Staining was accomplished by exposing the samples to the vapor of a 4% aqueous RuO_4 solution for 3 h.

Small-Angle X-ray Scattering (SAXS). SAXS experiments were performed at the wiggler beamline BL17B3 at the National Synchrotron Radiation Research Center (NSRRC), Taiwan. The incident X-ray beam was focused vertically by a spherical mirror and was monochromated to the energy of 12 keV by a Si(111) double-crystal monochromator (DCM). The wavelength of the X-ray beam was λ = 1.03 Å. The distance from the sample to the detector was 2749.7 mm, and the beam stop was a tantalum disk with a 4 mm diameter. SAXS data were collected using a two-dimensional area detector, and the sensitivity of the PSD was calibrated using a ^{55}Fe source before data collection. The calibration of the detector pixels in terms of scattering vector was made by linear regression over the positions of numerous orders of silver behenate's long period as the standard, with q_{max} set to 1.076 nm^{-1}. The intensity profiles were put in as the plot of scattering intensity (I) vs scattering vector, q ($q = (4\pi/\lambda)\sin(\theta/2)$, where θ is the scattering angle).

Results and Discussion

Preparations of Hydroxyl-Capped iPP by Selective Chain Transfer to Aluminum. Efforts for the preparations of OH-capped iPP via the selective chain transfer to aluminum reaction were examined by conducting isospecific propylene

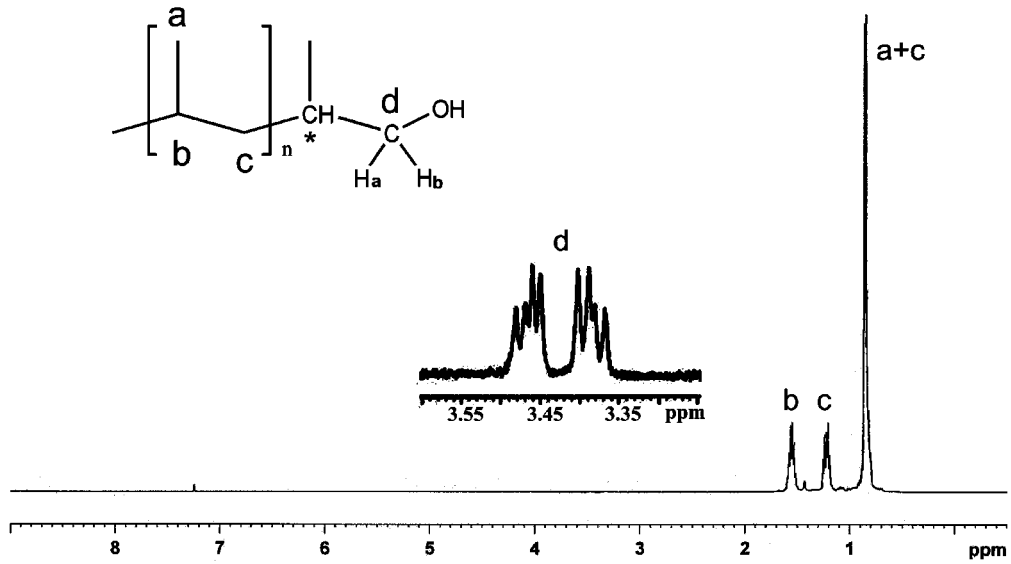

Figure 3. [1]H NMR spectra (500 MHz) of the OH-capped iPP (M_n = 5400 g/mol, M_w/M_n = 1.77; entry 19 of Table 1) (solvent, $CDCl_3$; temperature 60 °C).

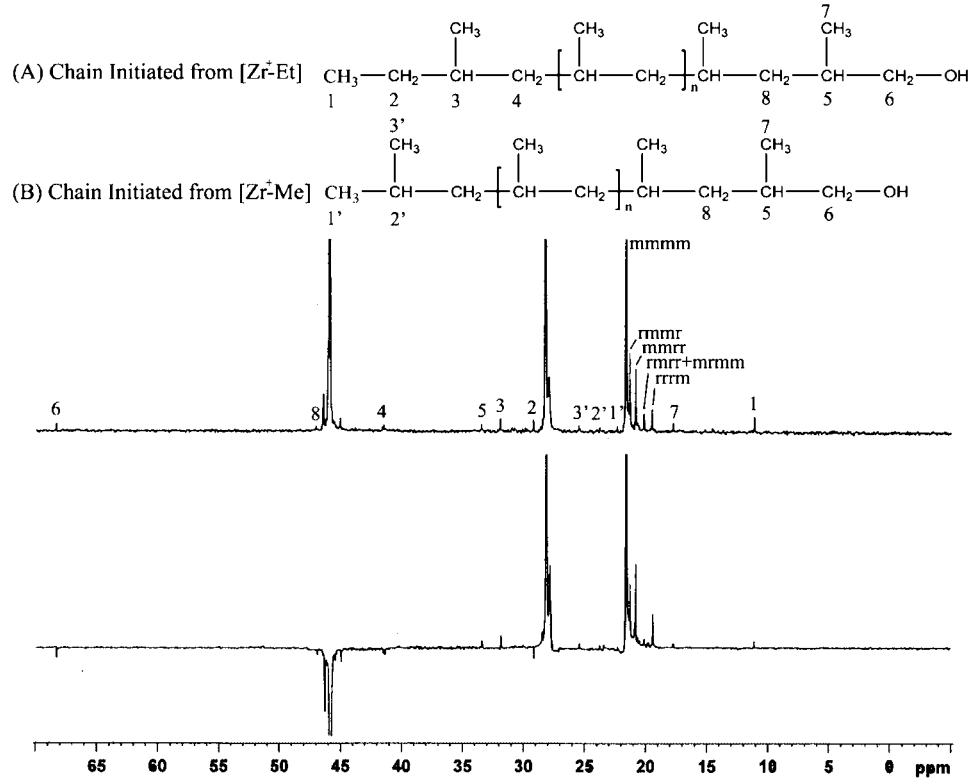

Figure 4. (a) [13]C and (b) [13]C (DEPT-135) NMR (500 MHz) spectra of the OH-capped iPP (M_n = 5400 g/mol, M_w/M_n = 1.77; entry 19 of Table 1) (solvent, $CDCl_3$; temperature 60 °C).

polymerization in the presence of various alkylaluminums (i.e., TMA, TEA, and TIBA) and isospecific *ansa*-metallocene complexes, including *rac*-$(Me)_2Si(Ind)_2ZrCl_2$ (I), *rac*-$(Me)_2C(Ind)_2$-$ZrCl_2$ (II), and *rac*-$C_2H_4(Ind)_2ZrCl_2$ (III). After the reaction, the polymer solution was in situ treated with O_2/H_2O_2 for converting the aluminum end group of iPP to the hydroxyl terminal group. The resulting polymer solution was then charged with excess methanol, leading to the deposition of iPPs as a white precipitate. [1]H and [13]C NMR spectra of the iPPs produced under these conditions were evaluated to determine the chain end structures. The results of the polymerization studies are summarized in Table 1.

There are four possible chain release pathways that lead to the generation of the iPPs with characteristic vinylidene, allyl, 2-butenyl, and hydroxyl end groups as illustrated in Scheme 2. The vinylidene chain end was generated form the primary insertion propylene unit, which underwent subsequent β-hydride elimination chain transfer. The 2-butenyl end group was formed from the secondary insertion propylene unit that underwent subsequent β-hydride elimination transfer. The hydroxyl end group was produced form the primary insertion propylene unit, which underwent chain transfer to aluminum so as to give aluminum-capped iPP as the preliminary reaction product; subsequently, the in situ oxidation of the resulting aluminum-

Scheme 3

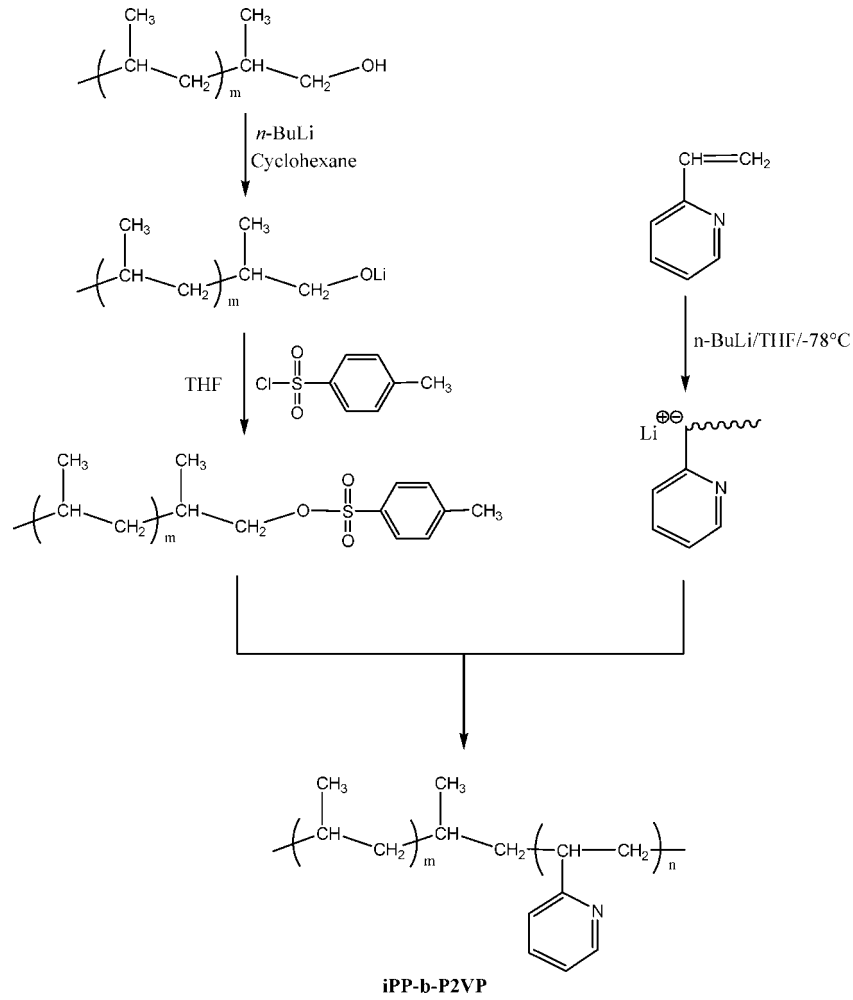

capped iPP with O_2/H_2O_2 by the method described in the experiment section led to the generation of OH-capped iPP. As shown in Table 1, mediating the isospecific propylene polymerization in the presence of catalysts I, II, and III using TMA as the chain transfer agent typically leads to the generation of iPPs containing three different chain-end structures, including vinylidene, 2-butenyl, and hydroxyl end groups. We are unable to detect any allyl end-capped iPP, which can be predominantly

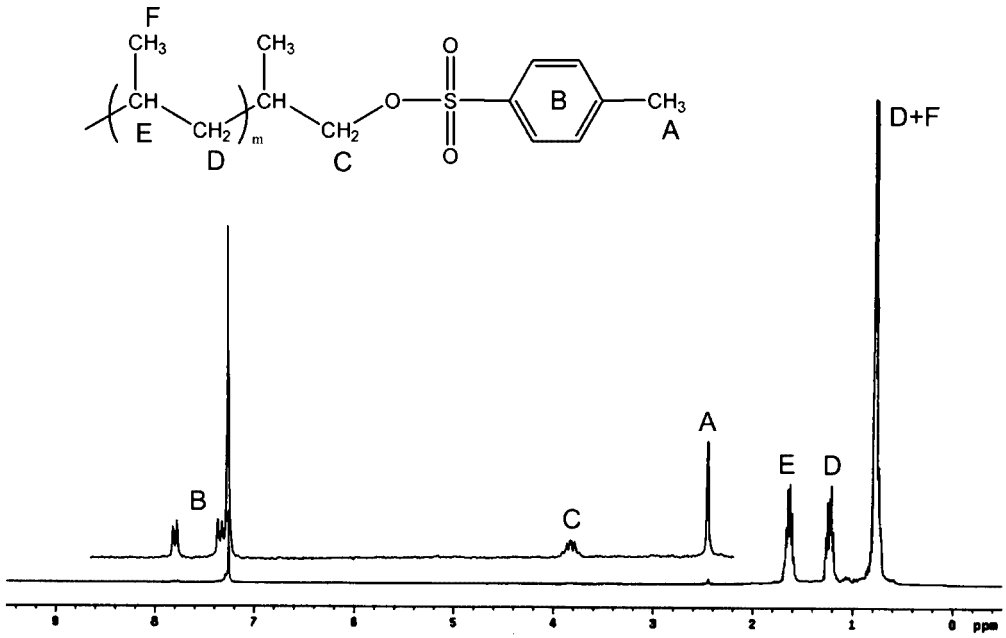

Figure 5. ^{1}H NMR spectra (500 MHz) of the tosyl group end-capped iPP (M_n = 2860 g/mol, M_w/M_n = 1.50) (solvent, $CDCl_3$; temperature 60 °C).

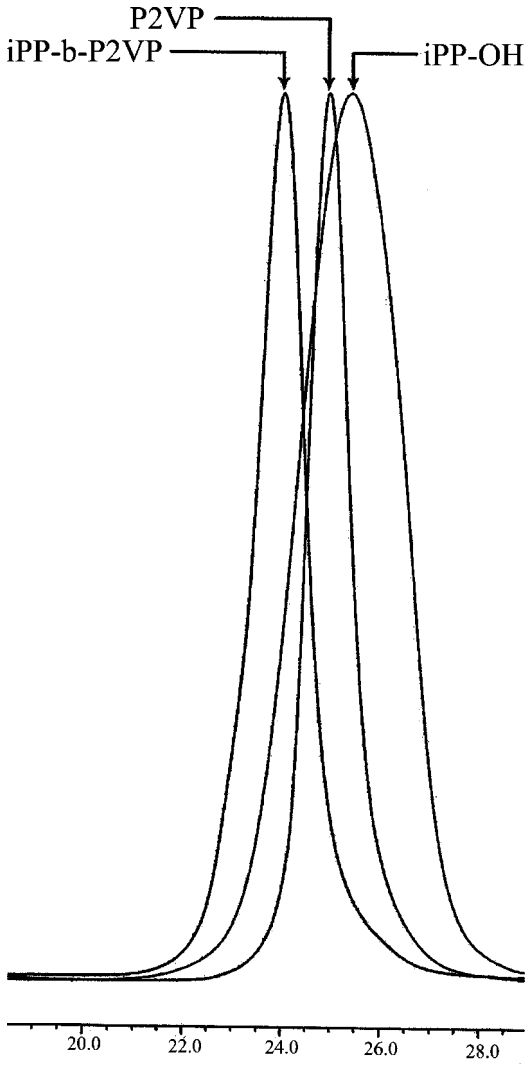

Figure 6. GPC curves comparison between (a) OH-capped iPP (M_n = 2820 g/mol, M_w/M_n = 1.50), (b) poly(2-vinylpyridine) (M_n = 4220 g/mol, M_w/M_n = 1.07), and (c) iPP-*b*-P2VP (M_n = 8020 g/mol, M_w/M_n = 1.10) (in 1,2,4-trichlorobenzene, at 135 °C).

generated via the β-methyl elimination chain releasing pathway by conducting propylene polymerization in the presence of bulky catalysts [e.g., $Cp^*_2ZrCl_2$ or $(Flu)_2ZrCl_2$; Flu = fluorenyl].[18] The absence of the allyl end-capped iPP under our polymerization conditions could be attributed to the fact that *ansa*-metallocenes I, II, and III do not have the sufficient bulky Cp ligands to promote the selective β-methyl elimination transfer.

Although iPPs prepared under TMA typically contained various chain-end structures that were generated by different chain releasing pathways,[9,19] the formation of OH-capped iPP via the chain transfer to the aluminum route was strongly dependent on the geometry of catalysts, structure of chain transfer agents (TMA, TEA, and TIBA), and the polymerization temperature. As shown in Table 1, β-hydride elimination transfer (producing vinylidene and 2-butenyl end groups) was the predominant chain releasing pathway when polymerization was conducted in the presence of *ansa*-metallocenes I and II. By contrast, mediating isospecific propylene polymerization in the presence of catalyst III shifts the chain releasing pathway from the predominant β-hydride elimination to mainly the chain transfer to aluminum. Similarly, replacing the TMA or TIBA with TEA led to the production of a substantially increasing amount of OH-capped iPP with a lower molecular weight as revealed by the comparative results (entries 1−3 and 4−6, 8−9 and 10−11, 12−14 and 15−17) listed in Table 1.[19] Besides, we also found that the formation of the OH-capped iPP can be highly dependent on the polymerization temperature. As revealed by the comparative results among entries 12−14 and among entries 15−17, reducing the polymerization temperature can effectively suppress the β-hydride elimination chain releasing pathway;[20,18a] thus, the iPPs generated at lower temperatures have lesser amounts of vinylidene and 2-butenyl end-capped iPP but have a higher ratio of the OH-capped iPP. The combination of these experimental results clearly indicates that the production of OH-capped iPP can be drastically enhanced by conducting isospecific propylene polymerization in the presence of the catalyst (III), at a lower polymerization temperature, and by using TEA as the chain transfer agent (Figure 1). It is important to note that the pure OH-capped iPP can be produced via the exclusive chain transfer to TEA by conducting the propylene polymerization at these conditions (entries 18−22), and this provides the pure OH-capped iPP for use as the end-functionalized prepolymer for the preparation of iPP-based stereoregular BCPs. Figure 2 shows the plot of polymer molecular weight versus [propylene]/[TEA] by conducting the propylene polymerization at 0 °C using *rac*-$C_2H_4(Ind)_2ZrCl_2$ as the catalyst and TEA as the chain transfer agent (entries 18−22 of Table 1). The nearly linear relationship between the molecular weight of iPPs and [propylene]/[TEA] ratio indicates that chain transfer to TEA (rate constant = k_{tr}) competes with the propylene chain propagation reaction. Since the degree of polymerization (X_n) follows the equation $X_n = k_p[\text{propylene}]/k_{tr}[\text{TEA}]$, the plot in Figure 2 provides the calculation of the chain transfer constant (k_{tr}/k_p = 1/25.61) for the generation of OH-capped iPP by the predominant chain transfer to TEA.

End-Group Analyses. End-group analyses provide the direct evidence of the chain releasing pathways and the successful preparation of pure OH-capped iPP. Figure 3 elucidates the ^1H NMR spectrum (with an inset of the expanded region and chemical shift assignments) of the OH-capped iPP (M_n = 5400 g/mol, M_w/M_n = 1.77; entry 19 of Table 1) isolated after the O_2/H_2O_2 treatment. The characteristics of the two sets of doublet coupling patterns ($J_{geminal}$ = 10.4 Hz and $J_{vicinal}$ = 6.5 Hz) correspond to the $-CH(CH_3)-CH_2-OH$ methylene proton absorptions situated in a diastereotopic environment. Figure 4 shows the ^{13}C (DEPT 135) NMR spectra (with an inset of the chemical shift assignments) of the lower molecular weight hydroxyl-capped iPP. The detailed chemical assignments are based on the structural information revealed in ^{13}C (DEPT 135), the two-dimensional ^{13}C and ^1H HMQC (Supporting Information) NMR spectra, and by comparison with prior NMR analyses of iPP.[21] These NMR spectra clearly revealed the selective generation of the OH-capped iPP as the pure reaction product, thus providing the OH-capped iPP as the structurally uniform end-functionalized prepolymer for use in the syntheses of iPP-based stereoregular BCPs.

Preparation of Stereoregular BCPs. Our study aims to develop a new synthetic method that leads to the successful preparation of stereoregular BCPs for self-assembly. Thus, the resulting stereoregular BCPs need to have a well-defined chemical structure, including the uniform chemical structure and molecular chain length, so as to afford uniform domain sizes in both polymer blocks for the formation of molecular self-aggregation.[22] In order to provide a suitable stereoregular BCP sample for self-assembly, the syntheses of stereoregular BCPs have to start from an end-functionalized prepolymer (OH-capped iPP) that has a narrow range of MWD.[15,16] Although end-functionalized prepolymers prepared via the metallocene route would typically have a broad range of MWD, a narrow MWD sample can be obtained by the fractionation of the broad MWD product through extraction processes.[15,16] Accordingly, a narrow

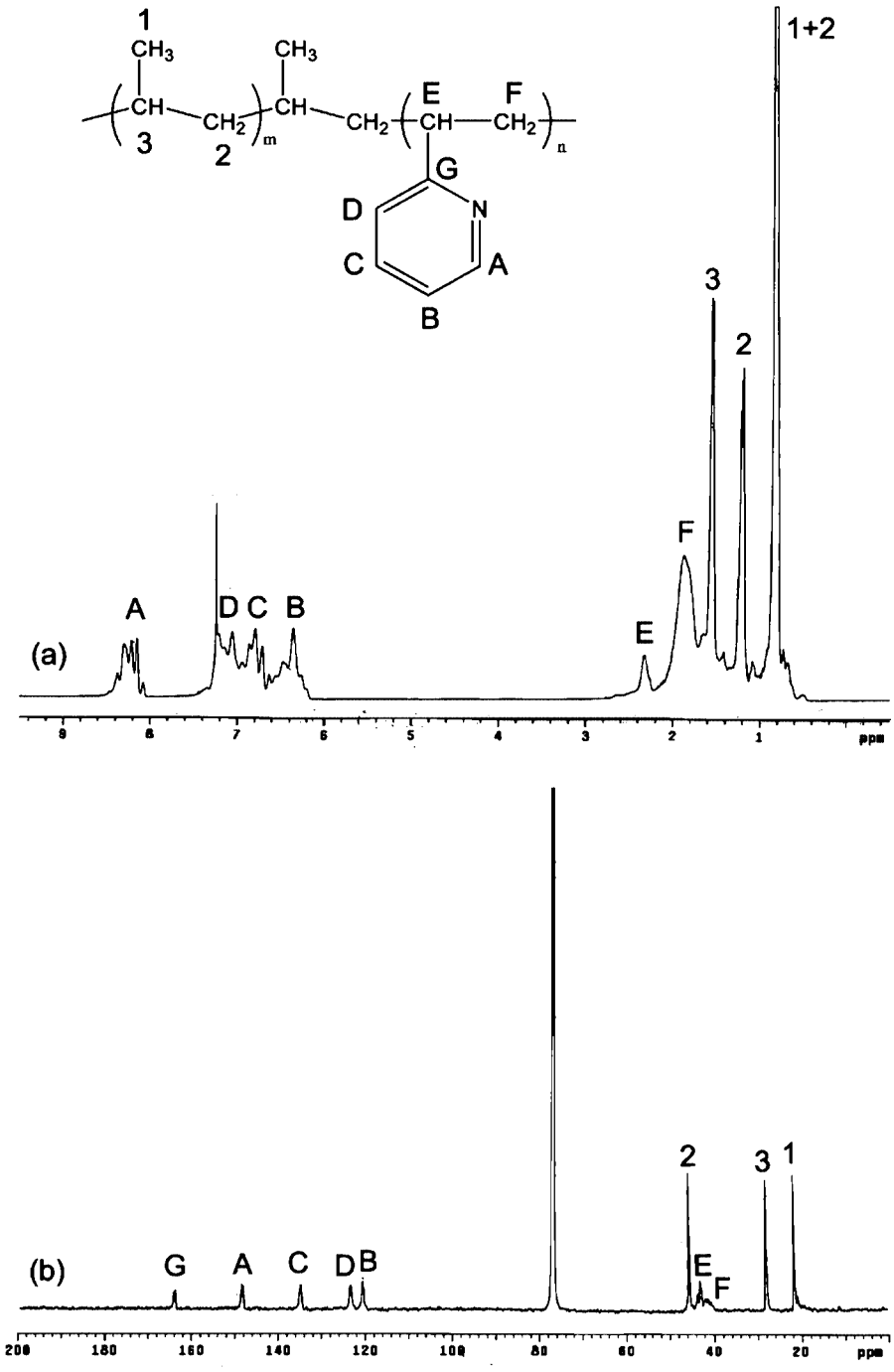

Figure 7. (a) ^{13}C (500 MHz) and (b) ^{1}H (500 Hz) NMR spectra of the iPP-*b*-P2VP (M_n = 8020 g/mol, M_w/M_n = 1.10) (solvent, $CDCl_3$; temperature 60 °C).

MWD sample of the OH-capped iPP [M_n = 2820 g/mol, MWD = 1.50, isotacticity (mmmm) = 76%], isolated from Soxhlet extraction of the broad MWD sample (M_n = 5400 g/mol, M_w/M_n = 1.77; entry 19 of Table 1) in THF, was used as the starting prepolymer for the construction of sPP-based stereoregular BCPs.

The detailed synthetic route for the preparation of the iPP-based stereoregular BCPs, iPP-*b*-P2VP, is illustrated in Scheme 3. As shown in this scheme, the hydroxyl group of the end-functionalized iPP was allowed to undergo tosylation reaction, which led to the successful generation of tosyl group end-capped iPP (M_n = 2860 g/mol, MWD = 1.50) with a good functional group conversion ratio as revealed by Figure 5. Consequently, the resulting tosyl group end-capped iPP was treated with an excessive amount of freshly prepared living anionic poly(2-vinylpyridine) (P2VP, M_n = 4220 g/mol, MWD = 1.07) to undergo anionic coupling. After the reaction, the pure stereoregular BCP (iPP-*b*-P2VP; M_n = 8020 g/mol, MWD = 1.10) was isolated through two consecutive Soxhlet extraction processes. The resulting polymer mixture was first extracted with methanol to remove the excess P2VP. The methanol-insoluble fraction was collected and was allowed to undergo the second Soxhlet extraction with heptane for the removal of the unused iPP (soluble in boiling heptane) so as to provide the pure iPP-*b*-P2VP (M_n = 8020 g/mol, MWD = 1.10). Figure 6compares the GPC elusion curves of the OH-capped iPP (M_n = 2800 g/mol, MWD = 1.50) and the P2VP (M_n = 4610, MWD = 1.07) with the iPP-*b*-P2VP (M_n = 8020 g/mol, MWD = 1.10). The successful preparation of the stereoregular BCPs can be further elucidated by NMR analyses. Figure 7 shows the ^{1}H

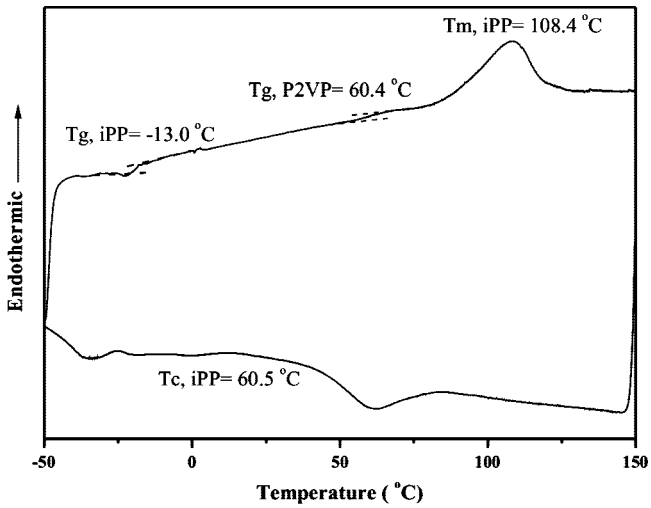

Figure 8. DSC thermograms of the iPP-*b*-P2VP.

and ^{13}C NMR spectra (with an inset of chemical structure and chemical shift assignments) of iPP-*b*-P2VP (M_n = 8020 g/mol, MWD = 1.10). The absence of any residual tosyl group absorption in both ^{1}H and ^{13}C NMR spectra (Figure 7a,b) clearly indicates the complete conversion of the tosyl end group and the generation of the pure iPP-*b*-P2VP sample for self-assembly.

Self-Assembly of Stereoregular BCPs. Since the iPP-*b*-P2VP is a semicrystalline BCP, to realize how crystallization affects the microphase-separated morphology is essential. To examine the mutual interaction between crystallization and microphase separation, the thermal behavior of synthesized iPP-*b*-P2VP was studied by DSC. Figure 8 shows the cooling and heating DSC thermograms of the iPP-*b*-P2VP. As shown, the temperatures of glass transition of the iPP block and the P2VP block in the iPP-*b*-P2VP can be clearly identified at −13.0 and 60.4 °C; the melting temperature of the iPP block is 108.4 °C. Also, the cooling thermogram exhibits an exothermic peak at 60.5 °C because of the crystallization of the iPP block. For self-assembly, bulk samples of the iPP-*b*-P2VP were prepared by melting the samples at 150 °C for 3 min and then quenching into liquid nitrogen. Although the crystallization of the iPP block did occur during cooling process and at ambient condition as well, the microphase-separated morphology remained due to the nanoscaled confinement for crystallization (see below for details).[23] As a result, the equilibrium ordered melt morphology was preserved for further structure identification. Subsequently, the quenched iPP-*b*-P2VP samples were microsectioned into a thickness of 40 nm for the TEM observation. Owing to the RuO_4 staining effect, the iPP and P2VP microdomains appeared as bright and dark regions, respectively. As shown in Figure 9a, the TEM image of the iPP-*b*-P2VP ($f_{iPP}^{v} = 0.40$) exhibits typical microphase-separated morphology with hexagonally packed cylinders. The 1D corresponding SAXS result for the iPP-*b*-P2VP examined at room temperature further confirmed the observed cylindrical nanostructure, with the scattering peaks being at q^* ratio of $1:\sqrt{4}:\sqrt{7}:\sqrt{9}$ (Figure 9b). The hexagonal packed cylinder nanostructure of the iPP-*b*-P2VP at ambient condition can thus be identified. Also, the typical lamellar nanostructure of the iPP-*b*-P2VP with symmetric composition can be found (not shown).

Shear-Induced Phase Transformation. As described, it is desirable to synthesize a specific three-dimensional bicontinuous gyroid phase. However, because of the narrow compositional window of gyroid phase in the phase diagram, it is difficult to fine-tune the synthesis of the iPP−P2VP samples with precise compositional fraction. An alternative way to acquire the formation of gyroid phase is to take advantage of the phase transformation from ordered phases such as lamellar phase or cylinder phase by shearing. The order−order transition from hexagonal cylinder phase to gyroid phase can be obtained via a large-amplitude oscillating shear at high temperature.[24] The bulk samples of the iPP−P2VP were subjected to a large-amplitude oscillating shear at 150 °C. Figure 10a,b shows TEM images of sheared iPP-*b*-P2VP, which forms the bicontinuous cubic gyroid phase. The "wagon wheel" morphology shown in Figure 9a performs approximately 3-fold symmetry corresponding to the [111] projection of the gyroid structure. Figure 10b shows the approximately 4-fold symmetry corresponding to the [100] projection of the gyroid structure. The corresponding SAXS profiles of the iPP-*b*-P2VP (Figure 10c) further prove the observed gyroid phase where the scattering peaks occur at q^* ratio of $\sqrt{3}:\sqrt{4}:\sqrt{7}:\sqrt{11}:\sqrt{24}$.[24,25] To eliminate the crystalline effect of iPP block, the SAXS experiments were also performed at 150 °C (above the melting of the iPP block), and the SAXS profiles were identical in q^* ratio. The in-situ SAXS results proved that the gyroid phase of the iPP-*b*-P2VP could be obtained via a large-amplitude oscillating shear at high temperature. The crystallization of the iPP block would not disturb the formation of nanostructure from the microphase separation of the iPP-*b*-P2VP.

It is known that the final morphology of the self-assembly of semicrystalline BCPs is strongly dependent on the experimental temperature, with respect to the order−disorder transition temperature (T_{ODT}), the crystallization temperature of the crystallizable block (T_c^c), and the glass transition temperature of amorphous block (T_g^a). For hard confinement with $T_{ODT} > T_g^a > T_c^c$, crystallization of a crystallizable block may occur within preexisting microdomains (MDs) created by microphase separation.[23,26] For systems with strong segregation strength, the crystalline growth would be confined to its melt morphology. Therefore, the number of possible conformations reduces because the restricted geometries imposed on crystallizing polymer materials are on a nanometer scale, which is approximately the length of a polymer chain in coil form. A rough estimate of the Flory interaction parameter χ can be obtained from the equation $\chi = (V_u/RT)(\delta_{iPP} - \delta_{P2VP})^2$, where the arbitrary reference volume V_u is conveniently selected as 100 cm^3/mol, and the solubility parameters are approximately 7.74 and 10.07 $(cal/cm^3)^{1/2}$ for iPP and P2VP, respectively.[27] At the experimental temperature window ranging from 25 to 150 °C, the χN values are approximately 78.0−110.7. In this study, the large-amplitude oscillating shearing was carried out at temperature ca. 150 °C; the χN value is approximately 78.0 (that is referred to intermediate segregation strength). Since the decrease of the segregation strength would make a reduction in packing frustration to compensate the increased surface area, the microphase-separated microdomains could be kinetically frustrated, such as shearing, and the order−order transition from cylinder phase to gyroid phase could thus be achieved.[24,28] As a result, a gyroid phase can be obtained by shearing. Furthermore, the isothermal crystallization temperature of the iPP blocks was conducted at 40 °C, which is lower than the T_g of P2VP blocks, 60.4 °C. Namely, the crystallization was occurred under the hard confinement ($T_{ODT} > T_g^a > T_c^c$). Although the crystallization of the iPP block did occur during isothermal crystallization process, the crystalline growth would be confined to its melt morphology in the system with relatively strong segregation strength (the χN value is approximately 105.4). It is noted that the microphase-separated morphology remains for crystallization under hard confinement with strong segregation strength, and the crystalline growth should be restricted within the confined contour due to the nanoscale confinement for crystallization.[23,26,29] For the crystallization of semicrystalline block copolymers with gyroid phase, the confined crystallization

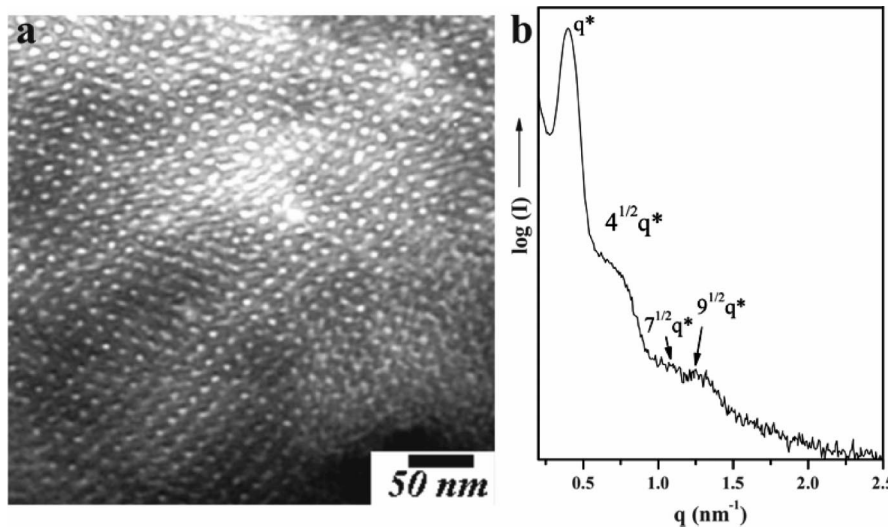

Figure 9. (a) TEM micrograph and (b) corresponding 1D SAXS profile of the iPP-*b*-P2VP.

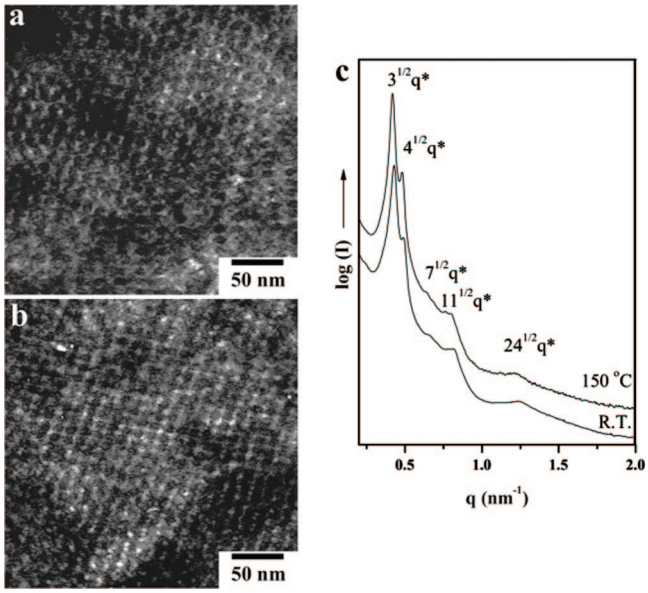

Figure 10. TEM micrographs: (a) 3-fold symmetry corresponding to [111] projection, (b) 4-fold symmetry corresponding to [100] projection of sheared iPP-*b*-P2VP, and (c) corresponding 1D SAXS profiles examined at room temperature and 150 °C.

seems to be in line with the common behavior. Consequently, the marriage of iPP block and P2VP block for the formation of the ordered three-dimensional bicontinuous phase might be an approach to enrich the functionality and complexities of the BCPs in the applications of nanotechnologies.

Conclusions

A new synthetic route that offers the first preparation of iPP-based stereoregular BCPs, iPP-*b*-P2VP, for self-assembly through the postpolymerization of end-functionalized iPP was demonstrated in this study. The end-functionalized iPP prepolymer (OH-capped iPP) was prepared by inducing selective chain transfer to alkylaluminum during isospecific polymerization of propylene in the presence of *ansa*-metallocene catalysts. Our results clearly indicated that the aluminum transfer efficiency is highly dependent on the geometry of the catalysts, the structure of alkyaluminum, and the polymerization temperature. Accordingly, pure OH-capped iPP can be generated by inducing the selective chain transfer to aluminum during isospecific propylene polymerization in the presence of *rac*-$C_2H_4(Ind)_2ZrCl_2$/MAO and TEA at a lower polymerization temperature. Subsequently, block copolymerization of the OH-capped iPP by postpolymerization affords the structurally well-defined iPP-based stereoregular BCPs (iPP-*b*-P2VP), which are able to self-assemble into consistent nanostructures. This study not only provides new synthetic methods for the preparation of various iPP-based stereoregular BCPs but also affords new insights into the chain releasing pathways during isospecific propylene polymerizations in the presence of alkylaluminums. Moreover, various microphase-separated nanostructures can be obtained by employing the iPP-based stereoregular BCPs for self-assembly. The self-assembled nanostructures from the BCPs with the marriage of the high solvent resistance of the crystallizing iPP block and the P2VP block as templated block for the inorganic/organic hybridization, especially a 3D bicontinuous gyroid, can be very appealing in the demands of new nanostructured system for a variety of applications.

Acknowledgment. J.-C. Tsai and R.-M. Ho acknowledge the National Science Council of Taiwan for the financial support for this research under contracts NSC-95-2216E-194-003 and NSC-95-2216E-110-009.

Supporting Information Available: ^{13}C and two-dimensional $^{1}H-^{13}C$ HMQC NMR spectra of the OH-capped iPP. This material is available free of charge via the Internet at http://pubs.acs.org.

References and Notes

(1) Recent reviews about block copolymers: (a) Lazzari, M.; Liu, G.; Lecommandoux, S. *Block Copolymers in Nanoscience*; Wiley-VCH Verlag GmbH & Co. KGaA: Weinheim, 2006. (b) Abetz, V.; Hadjichristidis, H.; Iatrou, H.; Pitsikalis, M.; Simon, P. F. W. *Adv. Polym. Sci.* **2005**, *189*, 1–124. (c) Hadjichristidis, N.; Pispas, S.; Floudas, G. *Block Copolymers: Synthetic Strategies, Physical Properties and Applications*; John Wiley and Sons: New York, 2003. (d) Alexandridis, P.; Lindman, B. *Amphiphilic Block Copolymers: Self-Assembly and Applications*; Elsevier: Amsterdam, 2000. (e) Calleja, F. J. B.; Roslaniec, J. *Block Copolymers*; Marcel Dekker: New York, 2000.

(2) (a) Bates, F. S.; Fredrickson, G. H. *Annu. Rev. Phys. Chem.* **1990**, *41*, 525–557. (b) Bates, F. S.; Fredrickson, G. H. *Phys. Today* **1999**, *52*, 32–38.

(3) (a) Zhu, L.; Mimnaugh, B. R.; Ge, Q.; Quirk, R. P.; Cheng, S. Z. D.; Thomas, E. L.; Lotz, B.; Hsiao, B. S.; Yeh, F.; Lin, L. *Polymer* **2001**, *42*, 912–9131. (b) Ryan, A. J.; Hamley, I. W.; Bras, W.; Bates, F. S. *Macromolecules* **1995**, *28*, 3860–3868. (c) Zhu, L.; Chen, Y.; Zhang, A.; Calhoun, B. H.; Chun, M.; Quirk, R. P.; Cheng, S. Z. D.; Hsiao, B. S.; Yeh, F.; Hashimoto, T. *Phys. Rev. B* **1999**, *60*, 10022–10031.

(4) (a) Ho, R.-M.; Chung, T.-M.; Tsai, J.-C.; Kuo, J.-C.; Hsiao, B. S.; Sics, I. *Macromol. Rapid Commum.* **2005**, *26*, 107–111. (b) Chung, T.-M.; Ho, R.-M.; Kuo, J.-C.; Tsai, J.-C.; Hsiao, B. S.; Sics, I. *Macromolecules* **2006**, *39*, 2739–2742. (c) Ho, R.-M.; Chiang, Y.-W.; Tsai, C.-C.; Lin, C.-C.; Ko, B.-T.; Huang, B.-H. *J. Am. Chem. Soc.* **2004**, *126*, 2704–2705.

(5) (a) Hatada, K.; Kitayama, T.; Ute, K.; Nishiura, T. *Macromol. Rapid Commun.* **2004**, *25*, 1447–1477. (b) Scherman, O. A.; Rutenberg, I. M.; Grubbs, R. H. *J. Am. Chem. Soc.* **2003**, *125*, 8515–8522.

(6) (a) Kandil, U.; Chung, T. C. *J. Polym. Sci., Part A: Polym. Chem.* **2005**, *43*, 1858–1872. (b) Dong, J. Y.; Wang, Z. M.; Hong, H.; Chung, T. C. *Macromolecules* **2002**, *35*, 9352–9359. (c) Lu, Y.; Hu, Y.; Wang, Z. M.; Manuas, E.; Chung, T. C. *J. Polym. Sci., Part A: Polym. Chem.* **2002**, *40*, 3416–3425. (d) Amin, S. B.; Marks, T. J. *J. Am. Chem. Soc.* **2007**, *129*, 2938–2953.

(7) Lin, W.-F.; Hsiao, T.-J.; Tsai, J.-C.; Chung, T.-M.; Ho, R.-M. *J. Polym. Sci., Part A: Polym. Chem.* **2008**, *46*, 4843–4856.

(8) (a) Koo, K.; Marks, T. *J. Am. Chem. Soc.* **1998**, *120*, 4019–4020. (b) Amin, S. B.; Marks, T. J. *J. Am. Chem. Soc.* **2007**, *129*, 10102–10103. (c) Fan, G.; Dong, J. Y.; Wang, Z.; Chung, T. C. *J. Polym. Sci., Part A: Polym. Chem.* **2006**, *44*, 539–548. (d) Lin, W. F.; Tasi, J. C. *J. Polym. Sci., Part A: Polym. Chem.* **2008**, *46*, 2167–2176. (e) Ringelberg, S. N.; Meetsma, A.; Hessen, B.; Teuben, J. H. *J. Am. Chem. Soc.* **1999**, *121*, 6082–6083.

(9) (a) Kang, K. K.; Shino, T.; Ikeda, T. *Macromolecules* **1997**, *30*, 1231–1233. (b) Quevedo-Sanchez, B.; Nimmons, F. J.; Coughlin, E. B.; Henson, M. A. *Macromolecules* **2006**, *39*, 4306–4316.

(10) Han, C. J.; Lee, M. S.; Byun, D. J.; Kim, S. Y. *Macromolecule* **2002**, *35*, 8923–8925.

(11) (a) Carvill, A.; Tritto, I.; Locatelli, P.; Sacchi, M. C. *Macromolecules* **1997**, *30*, 7056–7062. (b) Carvill, A.; Zetta, L.; Zannoni, G.; Sacchi, M. C. *Macromolecules* **1998**, *31*, 3783–3789. (c) Lieber, S.; Brintzinger, H. H. *Macromolecules* **2000**, *33*, 9192–9199. (d) Tynys, A.; Eilertsen, J. L.; Seppala, J. V.; Rytter, E. *J. Polym. Sci., Part A: Polym. Chem.* **2007**, *45*, 1364–1376. (e) Kim, I.; Zhou, J. M. *J. Polym. Sci., Part A: Polym. Chem.* **1999**, *37*, 1071–1082. (f) Kim, I.; Choi, C. S. *J. Polym. Sci., Part A: Polym. Chem.* **1999**, *37*, 1523–1539. (g) Kawahara, N.; Kojoh, S.; Matsuo, S.; Kaneko, H.; Matsugi, T.; Toda, Y.; Mizuno, A.; Kashiwa, N. *Polymer* **2004**, *45*, 2883–2888. (h) Naga, N.; Mizunuma, K. *Polymer* **1998**, *39*, 5059–5067. (i) Franceschini, F. C.; Tavares, T. T.; dos Santos, J. H. Z.; Ferreira, M. L.; Soares, J. B. P. *Marcromol. Mater. Eng.* **2006**, *291*, 279–287. (j) Franceschini, F. C.; Tavares, T. T.; Greco, P. P.; Galland, G. B.; dos Santos, J. H. Z.; Soares, J. B. P. *J. Appl. Polym. Sci.* **2005**, *95*, 1050–1055.

(12) Herrmann, W. A.; Rohrmann, J.; Herdtweck, E.; Spaleck, W.; Winter, A. *Angew. Chem., Int. Ed. Engl.* **1989**, *28*, 1511–1516.

(13) Nifant'ev, I. E.; Ivchenko, P. V. *Organometallics* **1997**, *16*, 713–715.

(14) Hasan, T.; Ioku, A.; Nishii, K.; Shiono, T.; Ikeda, T. *Macromolecules* **2001**, *34*, 3142–3145.

(15) Tsai, J.-C.; Kuo, J.-C.; Ho, R.-M.; Chung, T.-M. *Macromolecules* **2006**, *39*, 7520–7526.

(16) Hu, Y.; Krejchi, M. T.; Shah, C. D.; Myers, C. L.; Waymouth, R. M. *Macromolecules* **1998**, *31*, 6908–6916.

(17) (a) Resconi, L.; Piemontesi, F.; Gamurati, I.; Sudemijer, O.; Nifant'ev, I. E.; Ivchenko, P. V.; Kuz'mina, L. G. *J. Am. Chem. Soc.* **1998**, *120*, 2308–2321. (b) Collins, S.; Gauthier, W. J.; Holden, D. A.; Kuntz, B. A.; Taylor, N. J.; Ward, D. G. *Organometallics* **1991**, *10*, 2061–2068. (c) Zambelli, A.; Longo, P.; Grassi, A. *Macromolecules* **1989**, *22*, 2186–2189.

(18) (a) Resconi, L.; Piemontesi, F.; Franciscono, G.; Abis, L.; Fiorani, T. *J. Am. Chem. Soc.* **1992**, *114*, 1025–1032. (b) Resconi, L.; Jones, R. L.; Rheingold, A. L.; Yap, G. A. P. *Organometallics* **1996**, *15*, 998–1005.

(19) Kleinschmidt, R.; ven der Leek, Y.; Reffke, M.; Fink, G. *J. Mol. Catal. A* **1999**, *148*, 29–41.

(20) Liu, Z.; Somsook, E.; White, C. B.; Rosaaen, K. A.; Landis, C. R. *J. Am. Chem. Soc.* **2001**, *123*, 11193–11207.

(21) (a) Resconi, L.; Cavallo, L.; Fait, A.; Piemontesi, F. *Chem. Rev.* **2000**, *100*, 1253–1346. (b) Busico, V.; Cipullo, R.; Chadwick, J. C.; Modder, J. F.; Sudmeijer, O. *Macromolecules* **1994**, *27*, 7538–7543.

(22) Lynd, N. A.; Hillmyer, M. A. *Macromolecules* **2005**, *38*, 8803–8810.

(23) (a) Cohen, R. E.; Cheng, P. L.; Douzinas, K.; Kofinas, P.; Berney, C. V. *Macromolecules* **1990**, *23*, 324–327. (b) Hamley, I. W.; Fairclough, J. P. A.; Terrill, N. J.; Ryan, A. J.; Lipic, P. M.; Bates, F. S.; Towns-Andrews, E. *Macromolecules* **1996**, *29*, 8835–8843. (c) Quiram, D. J.; Register, R. A.; Marchand, G. R.; Adamson, D. H. *Macromolecules* **1998**, *31*, 4891–4898. (d) Chen, H.-L.; Wu, J. C.; Lin, T.-L.; Lin, J. S. *Macromolecules* **2001**, *34*, 6936–6944. (e) Zhu, L.; Cheng, S. Z. D.; Calhoun, B. H.; Ge, G.; Quirk, R. P.; Thomas, E. L.; Hsiao, B. S.; Yeh, F.; Lotz, B. *J. Am. Chem. Soc.* **2000**, *122*, 5957–5967. (f) Loo, Y. L.; Register, R. A.; Ryan, A. J. *Phys. Rev. Lett.* **2000**, *84*, 4120–4123.

(24) (a) Förster, S.; Khandur, A. K.; Zhao, J.; Bates, F. S.; Hamley, I. W.; Ryan, A. J.; Bras, W. *Macromolecules* **1994**, *27*, 6922–6935. (b) Khandur, A. K.; Förster, S.; Bates, F. S.; Hamley, I. W.; Ryan, A. J.; Bras, W.; Almdal, K.; Mortensen, K. *Macromolecules* **1995**, *28*, 8796–8806. (c) Hamersky, M. W.; Hillmyer, M. A.; Tirrell, M.; Bates, F. S.; Lodge, T. P.; Meerwall, E. D. *Macromolecules* **1998**, *31*, 5363–5370. (d) Hajduk, D. A.; Ho, R.-M.; Hillmyer, M. A.; Bates, F. S.; Almdal, K. *J. Phys. Chem. B* **1998**, *102*, 1356–1363. (e) Floudasm, G.; Vazaiou, B.; Schipper, F.; Ulrich, R.; Wiesner, U.; Iatrou, H.; Hadjichristidis, N. *Macromolecules* **2001**, *34*, 2947–2957. (f) Wang, C.-Y.; Lodge, T. P. *Macromolecules* **2002**, *35*, 6997–7006. (g) Schmidt, S. C.; Hillmyer, M. A. *J. Polym. Sci., Part B: Polym. Phys.* **2002**, *40*, 2364–2376.

(25) (a) Hajduk, D. A.; Harper, P. E.; Gruner, S. M.; Honeker, C. C.; Kim, G.; Thomas, E. L.; Fetters, L. J. *Macromolecules* **1994**, *27*, 4063–4075. (b) Bates, F. S.; Schulz, M. F.; Khandpur, A. K.; Förster, S.; Rosedale, J. H.; Almdal, K.; Mortensen, K. *Faraday Discuss.* **1994**, *98*, 7–18. (c) Vigild, M. E.; Almdal, K.; Mortensen, K.; Hamley, I. W.; Fairclough, J. P. A.; Ryan, A. J. *Macromolecules* **1998**, *31*, 5702–5716. (d) Loo, Y. L.; Register, R. A.; Ryan, A. J.; Dee, G. T. *Macromolecules* **2001**, *34*, 8968–8977.

(26) (a) Douzinas, K. C.; Cohen, R. E. *Macromolecules* **1992**, *25*, 5030–5035. (b) Cohen, R. E.; Bellare, A.; Drzewinski, M. A. *Macromolecules* **1994**, *27*, 2321–2323. (c) Khandpur, A. K.; Macosko, C. W.; Bates, F. S. *J. Polym. Sci., Part B: Polym. Phys.* **1995**, *33*, 247–252. (d) Liu, L.-Z.; Yeh, F.; Chu, B. *Macromolecules* **1996**, *29*, 5336–5345. (e) Hamley, I. W.; Fairclough, J. P. A.; Terrill, N. J.; Ryan, A. J.; Lipic, P. M.; Bates, F. S.; Towns-Andrews, E. *Macromolecules* **1996**, *29*, 8835–8843. (f) Hamley, I. W.; Fairclough, J. P. A.; Bates, F. S.; Ryan, A. J. *Polymer* **1998**, *39*, 1429–1437. (g) Weimann, P. A.; Hajduk, D. A.; Chu, C.; Chaffin, K. A.; Brodil, J. C.; Bates, F. S. *J. Polym. Sci., Part B: Polym. Phys.* **1999**, *37*, 2053–2068. (h) Zhu, L.; Cheng, S. Z.-D.; Calhoun, B. H.; Ge, Q.; Quirk, R. P.; Thomas, E. L.; Hsiao, B. S.; Yeh, F.; Lotz, B. *Polymer* **2001**, *42*, 5829–5839. (i) Sun, Y.-S.; Chung, T.-M.; Li, Y.-J.; Ho, R.-M.; Ko, B.-T.; Jeng, U.-S.; Lotz, B. *Macromolecules* **2006**, *39*, 5782–5788. (j) Sun, Y.-S.; Chung, T.-M.; Li, Y.-J.; Ho, R.-M.; Ko, B.-T.; Jeng, U.-S. *Macromolecules* **2007**, *40*, 6778–6781.

(27) (a) Rojo, E.; Fernández, M.; Munoz, M. E.; Santamaría, A. *Polymer* **2006**, *47*, 7853–7858. (b) Cui, L.; Wang, H.; Ding, Y.; Han, Y. *Polymer* **2004**, *45*, 8139–8146.

(28) (a) Matsen, M. W.; Bates, F. S. *Macromolecules* **1996**, *29*, 7641–7644. (b) Matsen, M. W.; Bates, F. S. *J. Chem. Phys.* **1997**, *106*, 2436–2448.

(29) (a) Fairclough, J. P. A.; Mai, S.-M.; Matsen, M. W.; Bras, W.; Messe, L.; Turner, S. C.; Gleeson, A. J.; Booth, C.; Hamley, I. W.; Ryan, A. J. *J. Chem. Phys.* **2001**, *114*, 5425–5431. (b) Hamley, I. W.; Castelletto, V.; Floudas, G.; Schipper, F. *Macromolecules* **2002**, *35*, 8839–8845. (c) Sun, L.; Zhu, L.; Ge, Q.; Quirk, R. P.; Xue, C. C.; Cheng, S. Z. D.; Hsiao, B. S.; Avila-Orta, C. A.; Sics, I.; Cantino, M. E. *Polymer* **2004**, *45*, 2931–2939.

MA8007288